

Final Revised KSU-1.docx

by Official Office

Submission date: 02-Dec-2023 12:29PM (UTC+0300)

Submission ID: 2209267620

File name: Final_Revised_KSU-1.docx (645.01K)

Word count: 5046

Character count: 29234

Effect of Adding (ZrO₂-ZnO) Nanopowder on the Polymer Blend (lamination and methyl vinyl silicone) in a Hybrid Nanocomposite Material

Abstract

A polymeric blend combines two or more polymers to form a new material with different physical properties. In this work, a base material consisting of a polymeric mixture was manufactured to improve its properties and then strengthened with nanoparticles (ZrO₂-ZnO) to develop a hybrid nanocomposite material, which has better properties than its constituent materials. Reinforcement material, i.e., (ZrO₂-ZnO) nanoparticles, were prepared using relaxation method. A polymeric resin mixture (lamination and methyl vinyl silicone) was prepared by adding methyl vinyl silicone to the lamination resin in different ratios (4%, 8%, 12%, and 16%). The mixture properties were studied through tensile, bending, shock, and hardness tests, and the optimal results were achieved for the 12% ratio. The resulting composite nanoparticles and their properties were studied using EDX, X-Ray, SEM, and PSA techniques. Finally, the nano-hybrid composite material was manufactured by choosing the optimal blend (i.e., 12%). It had the highest polymeric base material properties, and nanoparticles were added at different dosages (3%, 6%, 9%, and 12%). The resulting hybrid composite material properties were studied through different tests (tensile, flexural, impact, and hardness). The results showed that the binary composite nanoparticles improved the properties of the mixture for both sizes (30 nm and 89 nm) at all mixing ratios, compared to the control specimens (i.e., without any addition). The optimal results were obtained when 30nm particles were added and for all tests compared to samples reinforced with 89 nm particles. The optimal ratio of (ZrO₂-ZnO) was 9% wt 30 nm size, representing the best sample in terms of the resulting properties. It is recommended to use the sample with the 9% addition of (ZrO₂ - ZnO) wt with a granular size of (30 nm) in essential applications, including prosthetics (foot).

Keywords: Composite Nanopowders; sol-gel; relaxation; polymeric blend; medical applications

1. Introduction

Nanomaterials have opened the door wide for researchers to develop composite materials. Thus, a new class of composite materials emerged – nanocomposites. These are distinguishable from traditional composite materials in strength, durability, and excellent properties [1,2]. The discovery of nanomaterials led to an industrial revolution in all medical, engineering, electronic, civil, military, and space fields [3,4]. Nano oxides have taken a wide place in various applications because of their good properties, the most important of which are oxides of aluminum, zircon, zinc, calcium,

magnesium, and other oxides [5,6]. Among the most important applications are (strengthening materials, coatings, medical applications, and refractories) [7].

Many researchers have studied the development of composite materials and their components to improve their properties [8]. Arshian et al. [9] used zinc oxide nanoparticles added to (polyhydric silsesquioxane) and hybridized with the addition of (polylactic acid). Using XRD, the interaction of the particles with the polymer was observed. The tensile test results showed that the tensile strength increased significantly, and the increase in the contact angle proved the composite material had become hydrophobic. The antibacterial test further corroborated the antibacterial characteristics of the material. Kyung et al. [10] used fumed silica as an improved material for the thermal and mechanical properties of epoxy composites. The silica was treated with PDMS. The results showed that the silica treated with this material increased thermal stability and reduced thermal decomposition. It also increased the bending resistance compared to the composites reinforced with untreated silica. Hasanzadeh et al. [11] used PMMA as a matrix material after being dissolved and mixed with nanoparticles (TiO_2 , SiO_2 , and Al_2O_3) to strengthen it by specific weight ratios (0.5, 1, and 2%), Young's modulus and impact resistance were measured in addition to the Rockwell hardness. The results confirmed that the addition of nanomaterials significantly improved the mechanical properties. The improvement was 94% and 229% in the shock resistance of the TiO_2 -reinforced samples (by 1% and 2% reinforcement, respectively). Young's modulus and hardness also increased with the increase of different nanomaterials.

By using Fourier Transformed Infrared Spectroscopy (FTIR) and X-ray Diffraction (XRD) analyses, Xavier [12] developed NiO-ZrO₂ nanoparticles. Polyurethane (PU) was mixed with NiO-ZrO₂ nanoparticles, and the resulting polyurethane (PU)/NiO-ZrO₂ nanocomposite was applied as a coating on the steel specimens. Using scanning electrochemical microscopy (SECM), potentiodynamic polarisation investigations, and electrochemical impedance spectroscopy, the anticorrosion performance of the PU/NiO-ZrO₂ nanocomposite coating was investigated (EIS). According to EIS investigations, PU/NiO-ZrO₂ coating demonstrated a noticeable protective efficacy in natural seawater. Compared to PU coating, the PU/NiO-ZrO₂ SECM examination detected less current at the scratch of the coated surface. Surface morphological investigations (SEM/EDX) were used to analyze the surface characteristics and elemental composition of the coating samples. The mechanical characteristics of the nanocomposite and pure PU coatings demonstrated that mixed nanoparticles of metal oxide (NiO-ZrO₂) improved the mechanical and also corrosion protection characteristics of the polyurethane coating.

Sallal et al. [13] used (Al₂O₃-CaO) nanoparticles in various proportions (0.5–2 wt%) and a matrix of a polymeric blend consisting of 4% epoxy and 96% polyester. Mechanical tests were carried out on the samples that showed that the best incorporation percentage was 1.5 wt%. Zinc oxide-zirconium (IV) phosphate (ZnO-ZrP) nanocomposite was developed by Kaushal et al. [14] using the sol-gel technique at pH≈2. Thermal analysis, Fourier transform infrared spectroscopy, X-ray diffraction, energy dispersive X-ray spectroscopy, transmission electron microscopy, and scan electron microscopy were used to characterize it. Various characteristics of nanocomposites, including fixed charge density, perm selectivity, transport number, membrane potential, and ion exchange capacity, were investigated. The ion-exchange capacity of the nanocomposite ion exchange for Na⁺ ions was determined as 0.60 meq/g. It was investigated how adding ZnO nanoparticles affected the characteristics of the zirconium (IV) phosphate ion-exchange membrane. It is interesting to note that the nanocomposite showed some antibacterial action against the Gram-negative E. coli culture.

The research significance and novelty of the current work lie in the use of composite binary nanoparticles prepared by the sol-gel relaxation method and combined with this prepared polymeric mixture to manufacture a nano-hybrid composite material. Such materials have not been used earlier to prepare a composite material. This hybrid nanocomposite material can be used in prosthetic applications.

2. Experimental methods

2.1. Tests methods and devices

2.1.1. X-ray Diffraction (XRD)

X-ray examination is used to determine the crystal structure and chemical composition of materials through the diffraction of X-rays passing through the material. The type of device was (6000 - XRD) Shimatzu Company. The examination mechanism depends on observing the scattering of the intensity of the X-ray beam falling on the sample (X-rays consist of photons, and changing the path of the photons when they hit the electrons of the material leads to a change in the energy of the photon and this change indicates the type and composition of the material).

2.1.2. Scanning electron microscope (SEM and EDX)

The German device type (T-Scan) was used. The working principle depends on firing a beam of electrons on the surface of a sample coated with a thin metallic film, which in turn reflects the

electronic rays to a screen, giving an image of the sample surface in addition to the chemical composition. 94
95

2.1.3. Particle size analysis 96

Particle size analyzer type (Nanobrook 90 Plus) US was used. This device uses a monocular lens system to receive all the scattered and emitted signals from particles from nano to millimeters. 97
98
Using a high-quality lens produces a high-resolution image of diffused and low light to ensure the reception of all signals. 99
100

2.1.4. Combined mechanical testing 101

The device type (Larry - China) (DWD-50) was used for tensile, bending, and compression tests. 102
103
The samples were manufactured according to the ASTM standard.

2.1.5. Shore Hardness 104

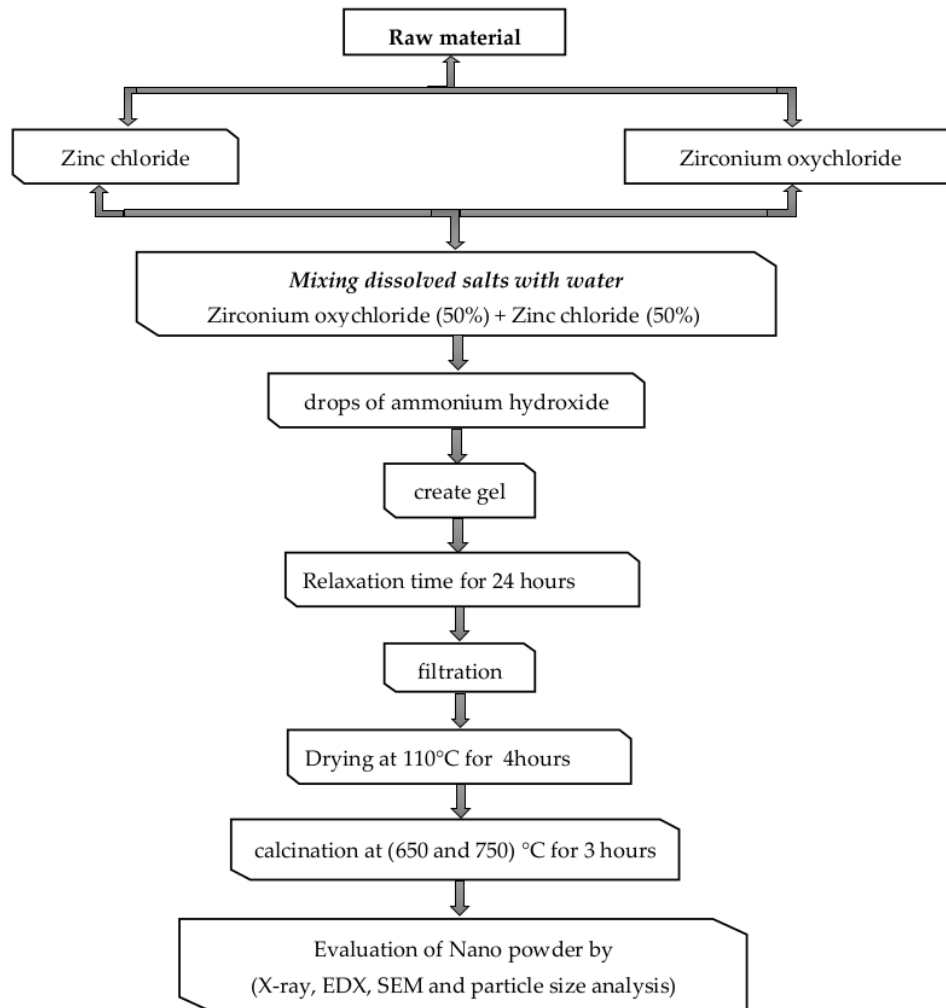
The Shore Dee device (Chinese origin) was used to measure the hardness of polymers based on the amount of immersion in the sample surface. 105
106

2.2. Raw materials 107

The materials used in the research to prepare the nano reinforcing and matrix materials were the polymeric blend including Zirconium oxychloride ($ZrCl_2O \cdot 8H_2O$) from Merck Company Germany, Zinc Chloride ($ZnCl_2$) from Thomas Baker, India and NH_4OH (Ammonium Hydroxide) from Thomas Baker, India. As for the polymers, lamination resin from Ottobock Company and methyl vinyl silicone resin from Elkem Company was used. 108
109
110
111
112

Figure 1 shows the steps for preparing nanoparticles. To prepare the composite ceramic nanoparticles, 1 M of each type of salt used in working with distilled water was dissolved to form two solutions to prepare for the subsequent mixing process. Both solutions were mixed equally (Zinc Chloride dissolved in distilled water and Zirconium Oxychloride dissolved in distilled water) for 70 minutes. After that, surfactant (sucrose) was added, and the mixing continued for another 20 minutes. Drops of Ammonium Hydroxide were added to form a gel. The formed gel was kept for (24 hours) at room temperature for a relaxation process that allowed sufficient time to complete the formation process of nanoparticles, sedimentation, and isolation of the minutes at the bottom of the beaker. After which, the filtered water was removed from the top of the gel container. The remaining substance was washed with warm distilled water several times. Then it was filtered on the filter paper to remove the remaining water. After filtration, the remaining material was dried at 113
114
115
116
117
118
119
120
121
122
123

23
110 °C for 4 hours. The dried material was calcinated at 650°C and 750°C for 3 hours. XRD, EDX, 124
and SEM of the resulting powder were carried out. 125



126

Figure 1: Flowchart showing the procedure for preparing the binary composite Nanopowders. 127

The second part of the work includes manufacturing a polymer blend consisting of two polymeric 128
materials (lamination and methyl vinyl silicone resin) and choosing the best ratio that gives the best 129
results through mechanical tests represented by checking (tensile, bending, hardness, and impact). 130
Different proportions (4, 8, 12, and 16 wt%) of methyl vinyl silicone resin to the lamination resin 131
were used. The selected proportions were taken from each material and mixed by a mechanical 132

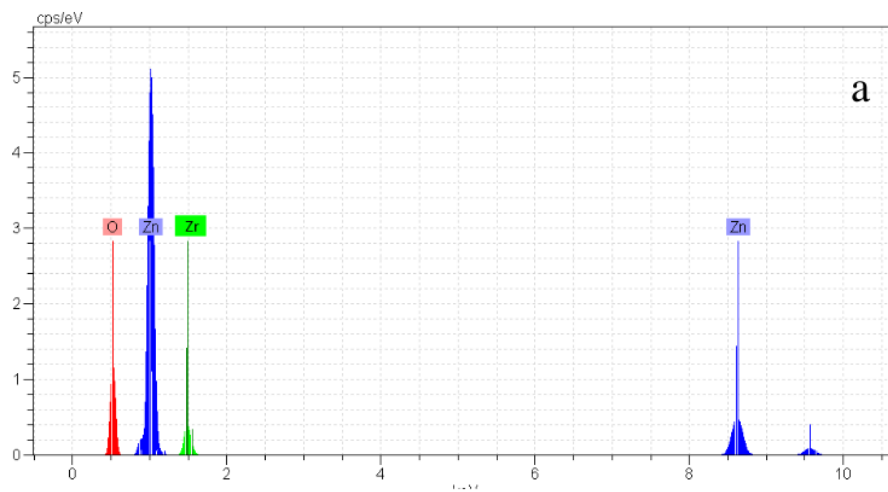
mixer for 15 minutes; then, the hardener was added. The samples were cast according to the standard specifications. The examination was done, and the best proportion was chosen to yield optimal test results. From the results, 12% methyl vinyl silicone and 88% lamination were selected as the optimal proportion, as it was to be considered a base material for manufacturing the nano-hybrid composite material. The nanopowder produced by the sol-gel method was combined in 3, 6, 9, and 12 % with the selected polymeric matrix material.

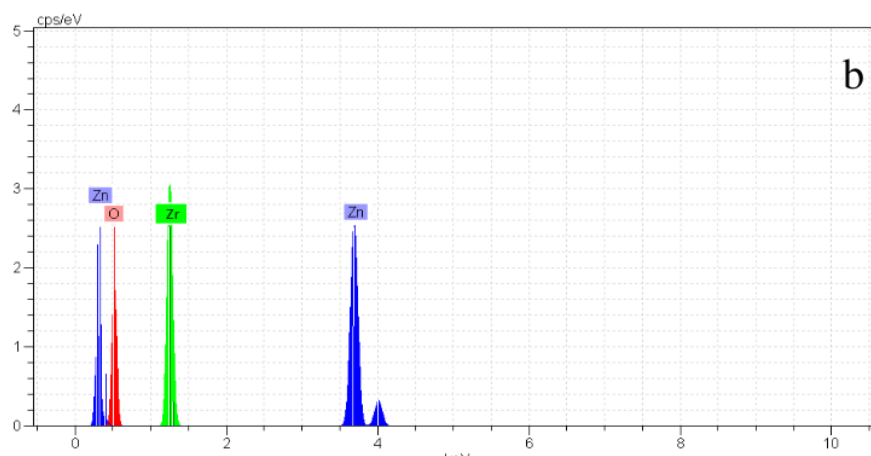
3. Result and discussion.

3.1. Tests for the preparation of binary composite Nanopowder.

3.1.1. EDX test

Figures 2a and b show the chemical composition of the calcined binary composite nanopowder at temperatures 650°C and 750°C. The resulting powder comprises zinc and zirconium oxides due to zinc and zirconium elements and oxygen, indicating oxide formation. There are no impurities within the composition, indicating the product purity.





147

Figure 2: a) the chemical composition of the calcined binary composite nanopowder at temperatures (650°C); b) the chemical composition of the calcined binary composite nanopowder at temperatures (750°C).

148

149

150

19

3.1.2. X-ray diffraction (XRD) test

151

Figure 3 shows the effect of temperature on the nanocomposite powder on the formation of zirconia phases; after that, calcination at temperature 650°C. Two phases of zirconia appeared, (t, m) and zinc oxide, according to JCPDS card no.s, respectively 17-0923, 37-1484, 36-1451. After calcination at 750 °C, one phase appeared for zirconia with zinc oxide according to JCPDS card no 17-0923 and 36-1451, respectively [15]. The monoclinic and tetragonal phases of zirconia at 650°C were observed, whereas only the tetragonal phase was found for zirconia at 750 °C. This disparity may be attributed to the relaxation mechanism and the sol-gel method used in the preparation process, giving a variety of phases resulting from a particular substance at different temperatures, in addition to the chemical composition resulting from mixing different materials to produce a mixture of oxides, which can be a catalyst in the formation of phases or reduction of their composition at certain temperatures [16].

152

153

154

155

156

157

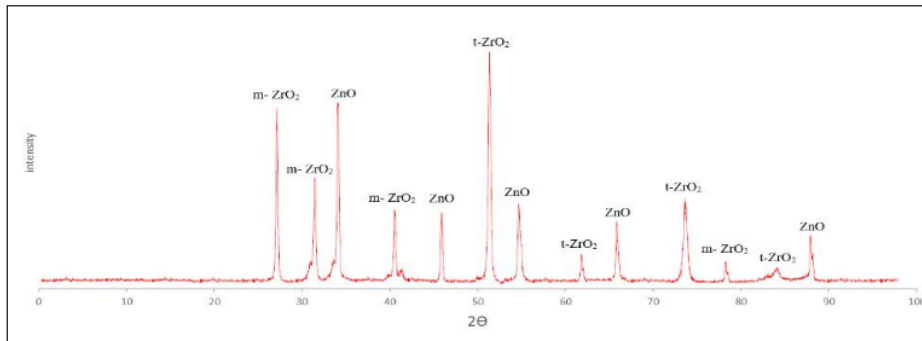
158

159

160

161

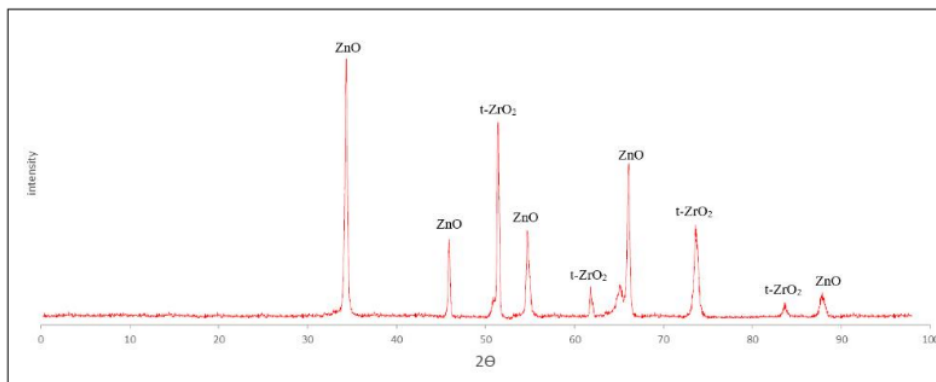
162



a

163

164



b

165

166

27

Figure 3: a) X-ray diffraction of the calcined binary composite nanopowder at temperatures (650°C), b) X-ray diffraction of the calcined binary composite nanopowder at temperatures (750°C).

167

168

169

3.1.3. PSA test.

170

10

The particle size analysis is shown in Figure 4. It is observed that the calcined binary nanocomposite powder at lower temperatures (650 °C) gave a particle size of 30 nm. The powder calcined at a higher temperature (750 °C) gave a particle size of 89 nm. Therefore, it is noted that the temperature affects the particle size due to the period required for cooling, as higher temperatures require more cooling time. Thus the growth of granules occurs, causing an increase in granular size [17].

171

172

173

174

175

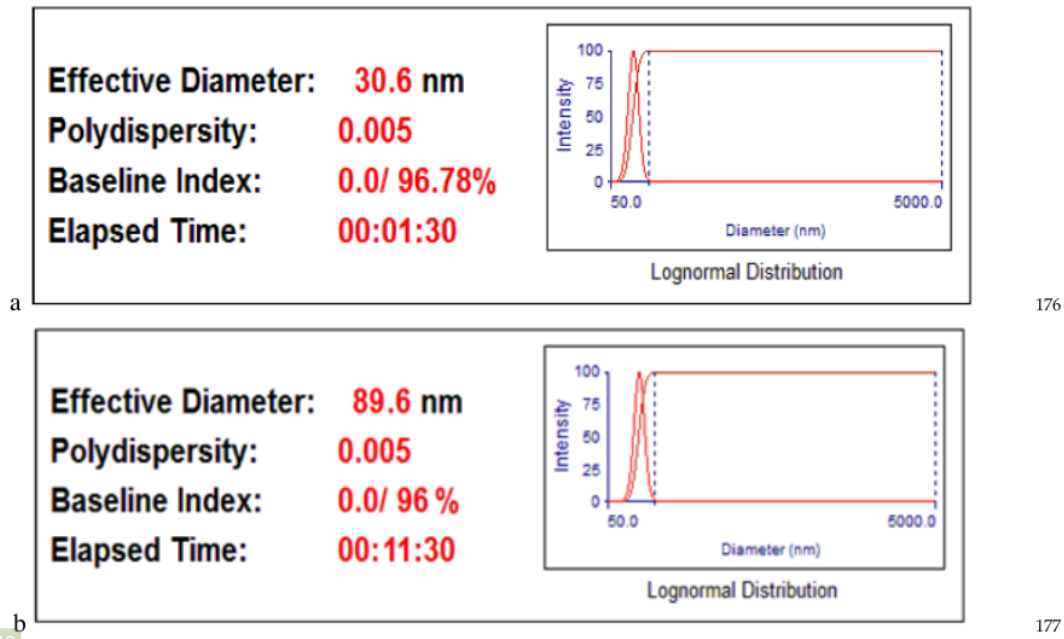
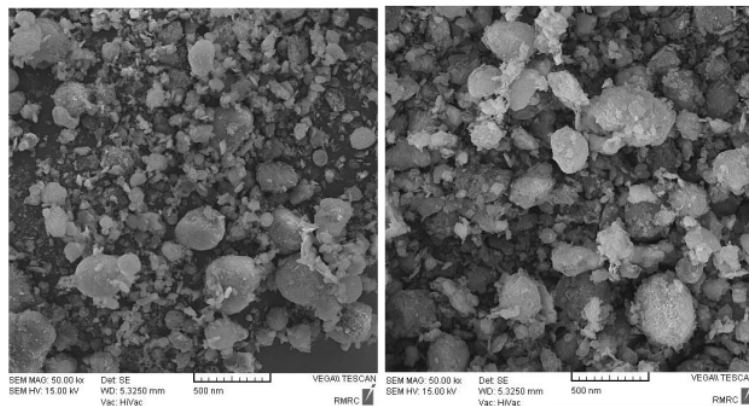


Figure 4: a) particle size analysis of the calcined binary composite nanopowder at temperatures (650°C), b) particle size analysis of the calcined binary composite nanopowder at temperatures (750°C).

3.1.4. SEM test

The particle shape and the aggregation of the calcination binary nanocomposite powder at 650°C and 750°C have been shown in Figure 5. The images show that the shape of the particles is almost spherical, giving the particles good dispersion and a high surface area. Particle agglomeration due to the small size of the particles, is also observed [18].



(a) (b) 187

Figure 5: a) SEM of the calcined binary composite nanopowder at (a) 650°C and (b) 750°C. 188

3.2. Mechanical tests on polymer blend 189

3.2.1. Tensile test 190

Figure 6(a) shows the curve resulting from the tensile test. It gives the maximum tensile strength 191
resulting from adding (methyl vinyl silicone resin) to (lamination resin) according to the selected 192
weight ratios (4, 8, 12, 16 wt%). The tensile test results showed that adding (methyl vinyl silicone 193
resin) to (lamination resin) increased tensile strength compared to pure material. The highest tensile 194
strength was obtained when adding (12%) methyl vinyl silicone resin, as (methyl vinyl silicone) 195
increased the bonding inside the substrate and led to an improvement in the mechanical properties 196
and, consequently, an increase in the strength [19]. The disparity in the mechanical properties of 197
the two polymers (when mixing in certain proportions) leads to enhanced properties to a certain 198
extent due to the activation of deformation mechanisms within the polymer network, causing an 199
improvement in the properties at a certain incorporation limit [20]. 200

3.2.2. Bending test 201

Figure 7(a) shows the curve resulting from the bending test. It gives the maximum bending re- 202
sistance from adding methyl vinyl silicone resin to lamination resin according to the selected 203
weight ratios (4,8,12,16 wt%). The bending test results showed that adding methyl vinyl silicone 204
resin to lamination resin led to increased bending resistance for all ratios compared to the pure 205
material. The highest bending strength was obtained when adding 12% methyl vinyl silicone. Me- 206
thyl vinyl silicone increased the resistance to bending well. Because of the activation of defor- 207
mation mechanisms within the polymer blend network resulting from the mismatch of mechanical 208
properties between the two polymers, so when mixing in certain proportions leads to an increase 209
in properties to a certain extent of addition. After exceeding this limit, the properties begin to de- 210
teriorate due to the change in the nature of deformation and bonding within the internal polymer 211
system [21]. 212

3.2.3. Impact test 213

The shock resistance and the impact test results are shown in Figure 8 (a). The results showed that 214
the polymeric mixture improved the impact resistance compared to the pure sample as the impact 215
resistance improved in general and for all weight ratios of the added resin. This indicates that the 216
polymeric mixture possessed good mechanical bonding and dispersing the absorbed energy during 217

5 impact and increasing the strength of the material, thus leading to an increase in the impact resistance of the polymeric mixture [22].

The impact property is variable because it is not considered a physical property of the material due to its dependence on the test conditions, sample geometry, test method, and certain other factors [23]. The increased toughness results from the good distribution of the polymer, which has the highest flexibility and plasticity within the polymeric blend, causing increased absorption of external energy applied to the material, and thus the ductility of the material increases [24].

3.2.4. Hardness test

The hardness and hardness test are shown in Figure 9 (a), where the Shore De hardness test showed that the polymeric mixture improved the hardness property. The Shore hardness values increased with the increase in the methyl vinyl silicone weight ratios and all ratios compared to the original sample. Resulting from the efficient distribution of the polymer, which has higher flexibility and plasticity within the polymer blend network, but the increase in these polymers leads to the deterioration of the mechanical properties due to their transformation into weak centers within the material, leading to the deterioration [25]. This indicates that the addition of methyl vinyl silicone increased the material's resistance to scratching and etching, resulting from the increase in hardness, which increases with the increase in the resistance and the mechanical bonding, the internal bonding between the bonds of the material [22].

3.3. Mechanical tests for hybrid nanocomposites reinforced by binary composite nanopowder.

3.3.1. Tensile test

Figure 6(b) represents the curve of weight ratios of the binary nanocomposite powder with the maximum tensile strength resulting from this addition to the polymeric blend. It is noted that the highest tensile strength was obtained at 9%, and its values were 78 MPa and 71 MPa for 30 nm and 89 nm particle sizes, respectively. It is seen that the particle size affects the tensile property. The tensile strength of nanocomposite reinforced with particle size 30 nm was higher than that of composite with particle size 89 nm. The particles helped strengthen the polymeric mixture by bonding the polymeric matrix with the nanoparticles [26,27]. In addition, the small size of the particles helped the good diffusion inside the polymer and, thus, a good distribution of loads within the nano-hybrid composite material [22,28]. The nanoparticles act according to the Hall-Petch effect as obstacles to the elastic and plastic deformations caused by the external loads [29]. Thus, these particles act as reinforcing materials for the polymeric material. In addition, they spread inside the

material better. The smaller the particle size, the greater the surface area, and thus the higher the wettability and the higher the bonding between the reinforcing material and matrix [30].

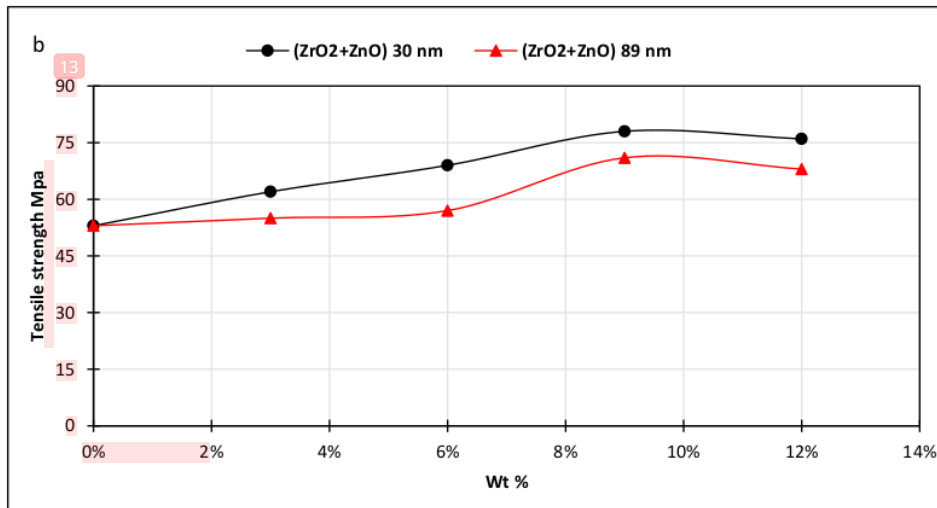
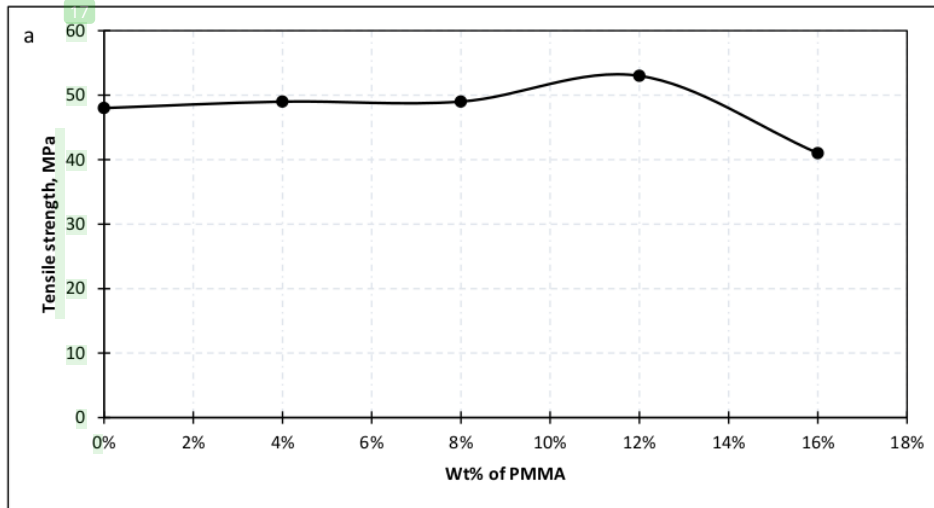
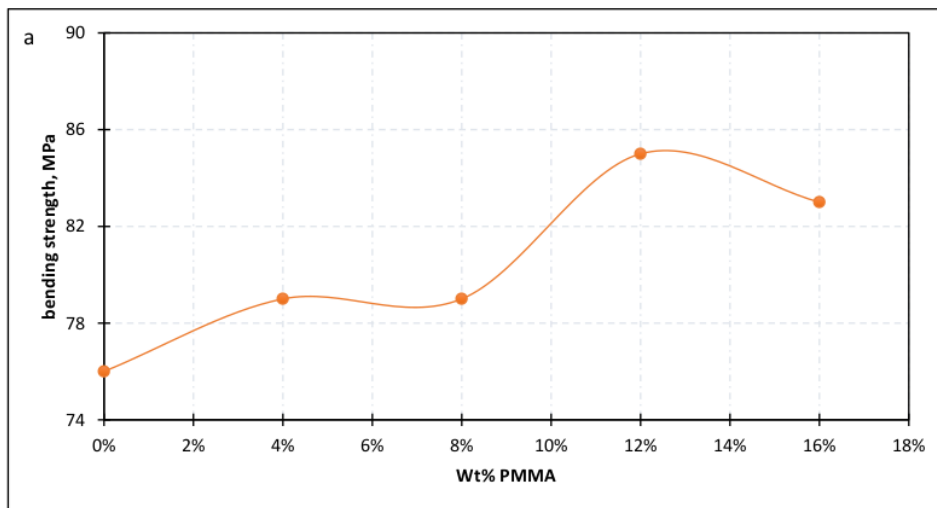


Figure 6: Maximum tensile strength a) From adding (methyl vinyl silicone resin) to (lamination resin), b) the polymeric blend reinforcement by binary nanocomposite powder.

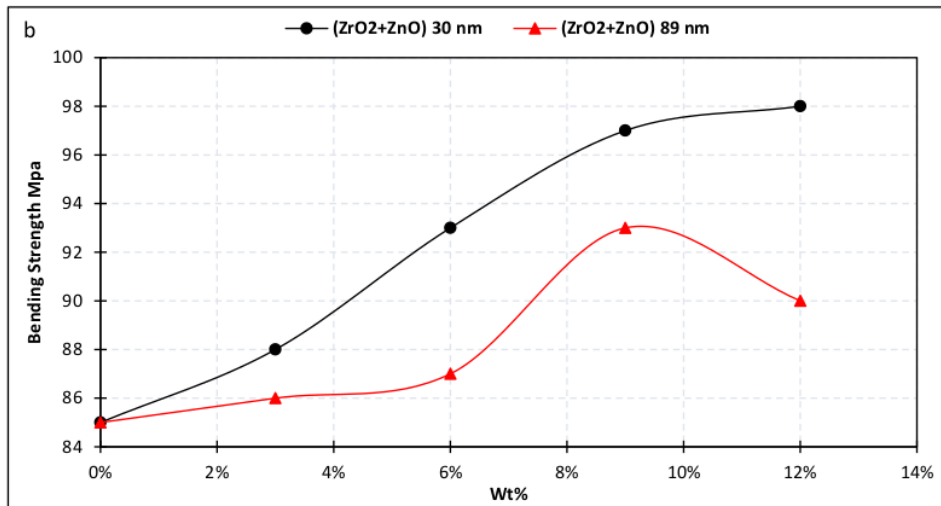
3.3.2. Bending test

Figure 7(b) shows the bending strength from adding the binary composite nanopowder to the polymeric mixture. The highest bending resistance was obtained at (12 and 9%), and its values were (98 and 93) MPa for each particle size 30 nm and 89 nm, respectively. It is also observed that the

particle size has good resistance to bending, especially at the particle size of 30 nm. The reinforcing material represented by the binary composite nanoparticles contributed to improving the bending resistance of the polymeric mixture through good diffusion inside the polymer matrix resulting from the small size of the reinforcement material. Thus, a good distribution of loads increases the strength of the interface separating the reinforcement and the base material within the nano-hybrid composite material [31,32]. The advantage of nanomaterials is that they have a large surface area according to the Hall-Petch effect, which gives them an advantage in diffusion and dispersion within other materials and thus leads to an increase in crosslinking within the polymer network and causes an increase in resistance and an improvement in properties [33,34]. However, exceeding certain incorporation limits leads to agglomeration, partially reducing the wettability and weakening the interface between the reinforcing material and the base material [35,36].



271



272

Figure 7: Maximum bending strength a) From dding (methyl vinyl silicone resin) to (lamination resin), b) the polymeric blend reinforcement by binary nanocomposite powder.

273

274

275

3.3.3. Impact test

276

Figure 8(b) signifies the curve of the weight ratios of the nano-reinforcing material added to the polymeric mixture with the impact resistance of the final hybrid composite material. It is noted from the screening results that the highest shock resistance was obtained at 12% at reinforcement by both 30 nm and 89 nm sizes, respectively. The material durability has improved due to the addition of nanoparticles, especially for 30 nm particle size. The toughness of the composite material improves whenever the linkage between the composite material components improves. This improvement comes from the strength of the interface between the base material and the reinforcing material, resulting from the large surface area. The interface and the reinforcing material increase the material's durability by dispersing external loads and reducing fracture growth [37].

277

278

279

280

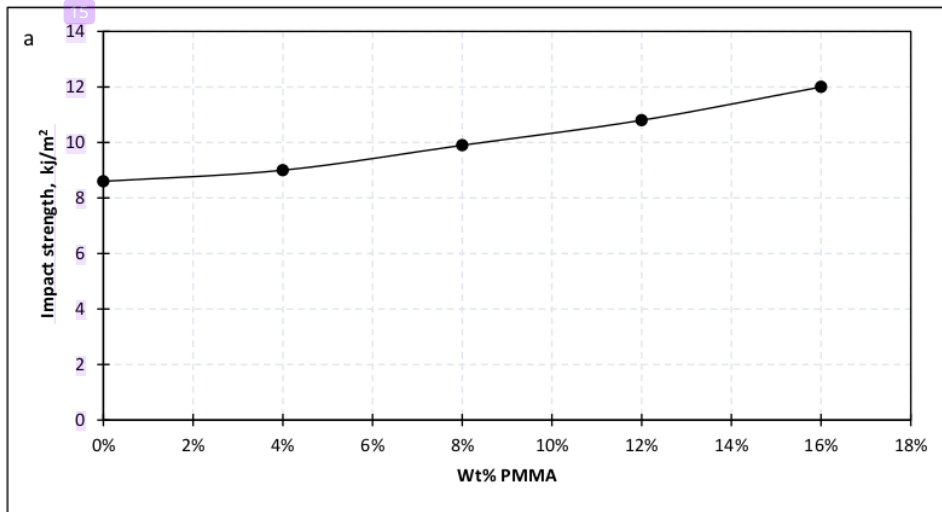
281

282

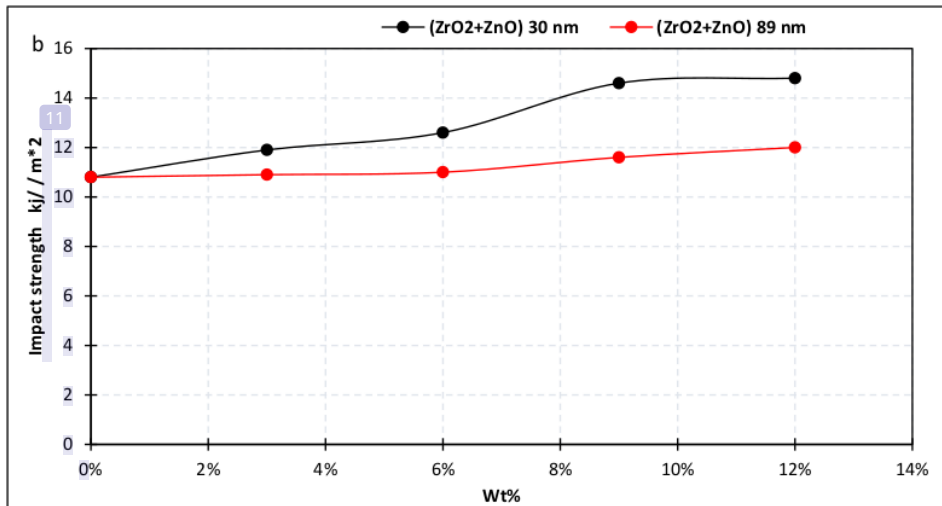
283

284

285



286



287

Figure 8: Impact strength a) From dding (methyl vinyl silicone resin) to (lamination resin), b) the polymeric blend reinforcement by binary nanocomposite powder.

288

289

3.3.4. Hardness test

290

Figure 9(b) shows the hardness test curve, represented by the relationship between the weight ratios of the nano-reinforcing material added to the polymeric mixture and the Shore D hardness of the final hybrid composite. The examination results showed that the hardness improved for all weight ratios and both sizes (30 and 89) nano. The hardness of the material gave higher values when adding particle size (30 nano). The hardness of the composite material increases when strengthening with

291

292

293

294

295

materials with a higher hardness than the hardness of the base material [27,32]. In addition, oxides are ceramic materials with high hardness, so adding them as a reinforcing material causes increased hardness [38,39]. Nanoparticles have a large surface area according to the Hall-Petch effect and thus lead to an increase in crosslinking within the polymer network and cause an increase in resistance and improvement in properties [40].

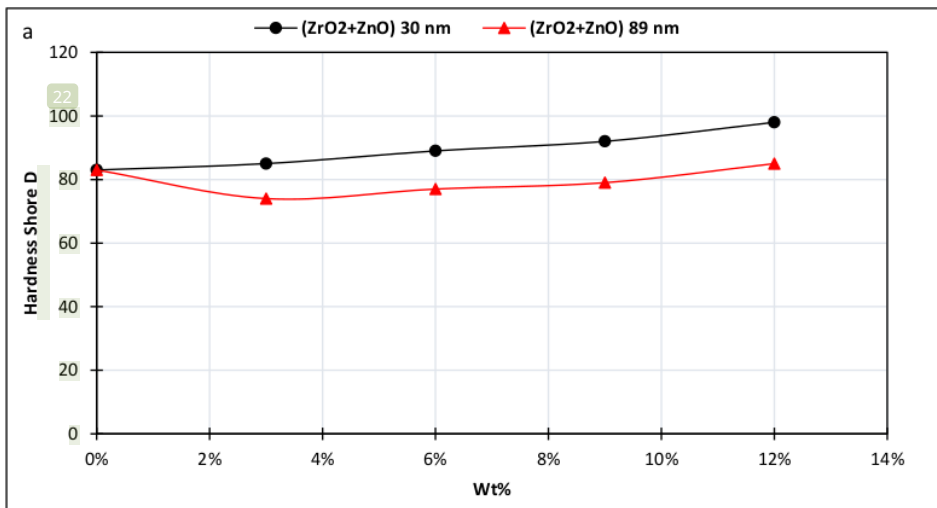
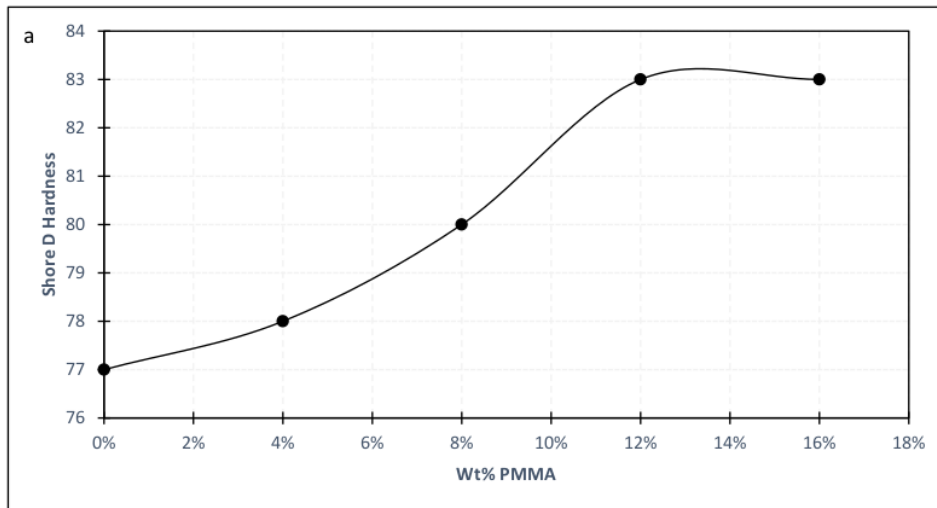


Figure 9: the hardness shore D a) From dding (methyl vinyl silicone resin) to (lamination resin),
b) the polymeric blend reinforcement by binary nanocomposite powder.

4. Conclusions

Based on the experimental work conducted with an objective of using composite binary nanoparticles prepared by the sol-gel relaxation method and combined with the prepared polymeric mixture to manufacture a nano-hybrid composite material, the following conclusions are reached:

- i. The results of the particle size analysis of the composite binary nanoparticles ($ZrO_2 + ZnO$) indicate that the temperature affects the particle size of resulting nanoparticles. At a temperature of 750 °C, a particle size of 89 nm was achieved compared to a particle size of 30 nm at a temperature of 650 °C. .
- ii. Examining the mechanical behavior of the prepared polymeric blend showed that the addition of 12% of methyl vinyl silicon is the optimum dosage. At 12% dosage, the results of the tests (tensile, bending, toughness, and hardness) were (53 MPa, 85 MPa, 10.6 KJ/m², 83) respectively.
- iii. The results of the mechanical tests showed that the optimal percentage addition for the nanoparticle ($ZrO_2 + ZnO$) was 9 wt % of the particle size 30nm, where the results of the tests tensile, bending, toughness, and hardness were determined as 78 MPa, 98 MPa, 14.6 KJ/m², and 96 respectively, compared to the control sample and the other samples to which the size was particle added was 89 nm.
- iv. Using the sample with the 9 wt % addition of ($ZrO_2 + ZnO$) with a 30 nm particle size is recommended in important applications, including prosthetics (foot).

Funds: None

Conflict of interest: The authors declare no conflict of interest to any party.

References

- [1] N.S. Radhi, N.M. Sahi, Z. Al-Khafaji, Investigation Mechanical and Biological Properties of Hybrid PMMA Composite Materials as Prosthesis Complete Denture, Egyptian Journal of Chemistry. (2022). <https://doi.org/10.21608/EJCHEM.2022.110545.5034>.
- [2] M. Hamad, I.A. Sarhan, Effect of Nano-Clay on Lightweight Self-Compacting Concrete Behavior, Knowledge-Based Engineering and Sciences. 2 (2021) 1–22.
- [3] A. Hanif, Z. Lu, P. Parthasarathy, D. Hou, Z. Li, G. Sun, Strength and hydration attributes of cement pastes containing nano titania and cenosphere, Advances in Cement Research. 32 (2020) 557–572. <https://doi.org/10.1680/jadcr.19.00015>.
- [4] S.A. Basilio, L. Goliatt, Gradient Boosting Hybridized with Exponential Natural Evolution Strategies for Estimating the Strength of Geopolymer Self-Compacting Concrete, Knowledge-Based Engineering and Sciences. 3 (2022) 1–16.
- [5] Z.M. Abed Janabi, H.S. Jaber Alsalami, Z.S. Al-Khafaji, S.A. Hussien, Increasing of the corrosion resistance by preparing the trivalent nickel complex, Egyptian Journal of Chemistry. (2021). <https://doi.org/10.21608/EJCHEM.2021.100733.4683>.

-
- [6] K.M. Abed, N.S. Radhi, A.H. Jasim, Z.S. Al-Khafaji, S. Radhi, S.A. Hussien, Study the effect of adding zirconia particles to nickel–phosphorus electroless coatings as product innovation on stainless steel substrate, *Open Engineering*. 12 (2022) 1038–1045. <https://doi.org/10.1515/eng-2022-0364>.
- [7] N.D. Fahad, N.S. Radhi, Z.S. Al-Khafaji, A.A. Diwan, Surface modification of hybrid composite multilayers spin cold spraying for biomedical duplex stainless steel, *Heliyon*. (2023). <https://doi.org/10.1016/j.heliyon.2023.e14103>.
- [8] H.A. Sallal, M.S. Radhi, M.H. Mahboba, Z. Al-Khafaji, Impact of embedded sol-gel synthesized triple composites on polymer's mechanical properties., *Egyptian Journal of Chemistry*. (2022). <https://doi.org/10.21608/ejchem.2022.154630.6684>.
- [9] M. Arshian, S. Estaji, M.I. Tayouri, S.R. Mousavi, S. Shojaei, H.A. Khonakdar, Poly (lactic acid) films reinforced with hybrid zinc oxide-polyhedral oligomeric silsesquioxane nanoparticles: Morphological, mechanical, and antibacterial properties, *Polymers for Advanced Technologies*. 34 (2023) 985–997.
- [10] K.-M. Kim, H. Kim, H.-J. Kim, Enhancing Thermo-Mechanical Properties of Epoxy Composites Using Fumed Silica with Different Surface Treatment, *Polymers*. 13 (2021) 2691.
- [11] R. Hasanzadeh, S. Rashmadi, H. Memari, Experimental investigation of mechanical properties of PMMA nanocomposites containing various contents of prevalent nanofillers from multi-criteria decision analysis point of view, *Journal of Mechanics*. 34 (2018) 461–468.
- [12] J.R. Xavier, Electrochemical and mechanical investigation of newly synthesized NiO-ZrO2 nanoparticle-grafted polyurethane nanocomposite coating on mild steel in chloride media, *Journal of Materials Engineering and Performance*. 30 (2021) 1554–1566.
- [13] H.A. Sallal, A.A. Abdul-Hameed, F. Othman, Preparation of Al₂O₃/MgO Nano-Composite Particles for Bio-Applications, *Engineering and Technology Journal*. 38 (2020) 586–593.
- [14] S. Kaushal, P.K. Sharma, S.K. Mittal, P. Singh, A novel zinc oxide–zirconium (IV) phosphate nanocomposite as antibacterial material with enhanced ion exchange properties, *Colloids and Interface Science Communications*. 7 (2015) 1–6.
- [15] P. Basnet, D. Samanta, T. Inakhunbi Chanu, J. Mukherjee, S. Chatterjee, Assessment of synthesis approaches for tuning the photocatalytic property of ZnO nanoparticles, *SN Applied Sciences*. 1 (2019) 1–13.
- [16] A. Taavoni-Gilan, E. Taheri-Nassaj, H. Akhondi, The effect of zirconia content on properties of Al₂O₃–ZrO₂ (Y₂O₃) composite nanopowders synthesized by aqueous sol–gel method, *Journal of Non-Crystalline Solids*. 355 (2009) 311–316.
- [17] J.A. Garibay'Alvarado, S.Y. Reyes-López, Sol–Gel Ceramics for SEIRAS and SERS Substrates, *Crystals*. 11 (2021) 439.
- [18] A. Bumajdad, A.A. Nazeer, F. Al Sagheer, S. Nahar, M.I. Zaki, Controlled synthesis of ZrO₂ nanoparticles with tailored size, morphology and crystal phases via organic/inorganic hybrid films, *Scientific Reports*. 8 (2018) 1–9.
- [19] K. Soygun, S. Şimşek, E. Yılmaz, G. Bolayır, Investigation of mechanical and structural properties of blend lignin-PMMA, *Advances in Materials Science and Engineering*. 2013

- (2013). 383
- [20] M.S. Goyat, A. Hooda, T.K. Gupta, K. Kumar, S. Halder, P.K. Ghosh, B.S. Dehiya, Role of 384
non-functionalized oxide nanoparticles on mechanical properties and toughening 385
mechanisms of epoxy nanocomposites, *Ceramics International*. 47 (2021) 22316–22344. 386
- [21] C. Zhang, L. Liu, Exploring the role of employability: the relationship between health- 387
promoting leadership, workplace relational civility and employee engagement, *Management 388
Decision*. 61 (2023) 2582–2602. 389
- [22] M.H. Mahboba, H.A. Sallal, F.H. Ali, Effect of particles size of zirconia on the mechanical 390
behavior of the polymer blend, in: *AIP Conference Proceedings*, AIP Publishing LLC, 2020: 391
p. 20310. 392
- [23] R. Molaei, A. Fatemi, N. Sanaei, J. Pegues, N. Shamsaei, S. Shao, P. Li, D.H. Warner, N. 393
Phan, Fatigue of additive manufactured Ti-6Al-4V, Part II: The relationship between 394
microstructure, material cyclic properties, and component performance, *International 395
Journal of Fatigue*. 132 (2020) 105363. 396
- [24] M. Amin, M. Ali, Polymer nanocomposites for high voltage outdoor insulation applications, 397
Rev. Adv. Mater. Sci. 40 (2015) 276–294. 398
- [25] D. Thomas, G. Ding, Comparing the performance of brick and timber in residential 399
buildings–The case of Australia, *Energy and Buildings*. 159 (2018) 136–147. 400
- [26] D.M.T. Mustafa, S. Rostam, S.B. Aziz, A comparative study on structural, morphological, 401
and tensile properties of binary and ternary epoxy resin-based polymer nanocomposites, 402
Advances in Materials Science and Engineering. 2020 (2020). 403
- [27] S.A. Abdulrahman, Q.A. Hamad, J.K. Oleiwi, Investigation of Some Properties for 404
Laminated Composite Used for Prosthetic Socket, *Engineering and Technology Journal*. 39 405
(2021) 1625–1631. 406
- [28] S.I. Salih, J.K. Oleiwi, Q.A. Hamad, Studying the Tensile Properties and Morphology Test 407
for the Self Cured PMMA Resin of Prosthetic Complete Denture, *The Iraqi Journal For 408
Mechanical And Material Engineering, Special Vol., Part II*. (2015) 508–522. 409
- [29] E. TAMBORINI, *Métallurgie colloïdale: structure et propriétés mécaniques d'un système 410
colloïdal modèle comme un analogue de polycristaux atomiques*, (2012). 411
- [30] B. Muralidhara, S.P.K. Babu, B. Suresha, Studies on mechanical, thermal and tribological 412
properties of carbon fibre-reinforced boron nitride-filled epoxy composites, *High 413
Performance Polymers*. 32 (2020) 1061–1081. 414
- [31] S.I. Salih, J.K. Oleiwi, Q.A. Hamad, Comparative study the flexural properties and impact 415
strength for PMMA reinforced by particles and fibers for prosthetic complete denture base, 416
The Iraqi Journal for Mechanical and Material Engineering. 15 (2015) 288–307. 417
- [32] D. Matykievicz, Hybrid epoxy composites with both powder and fiber filler: a review of 418
mechanical and thermomechanical properties, *Materials*. 13 (2020) 1802. 419
- [33] B.S. Murty, P. Shankar, B. Raj, B.B. Rath, J. Murday, *Textbook of nanoscience and 420
nanotechnology*, Springer Science & Business Media, 2013. 421
- [34] S.V.N.T. Kuchibhatla, A.S. Karakoti, D. Bera, S. Seal, One dimensional nanostructured 422
materials, *Progress in Materials Science*. 52 (2007) 699–913. 423
- [35] A. Khosla, H.T.A. Awan, K. Singh, R. Walvekar, Z. Zhao, A. Kaushik, M. Khalid, V. 424

-
- Chaudhary, Emergence of MXene and MXene–Polymer Hybrid Membranes as Future- 425
Environmental Remediation Strategies, *Advanced Science*. (2022) 2203527. 426
- [36] E.O. Olakanmi, R.F. Cochrane, K.W. Dalgarno, A review on selective laser 427
sintering/melting (SLS/SLM) of aluminium alloy powders: Processing, microstructure, and 428
properties, *Progress in Materials Science*. 74 (2015) 401–477. 429
- [37] S.A. Mechi, M. Al-Waily, Impact and Mechanical Properties Modifying for Below Knee 430
Prosthesis Socket Laminations by using Natural Kenaf Fiber, in: *Journal of Physics:* 431
Conference Series, IOP Publishing, 2021: p. 12168. 432
- [38] T.A. Nguyen, Q.T. Nguyen, T.P. Bach, Mechanical properties and flame retardancy of 433
epoxy resin/nanoclay/multiwalled carbon nanotube nanocomposites, *Journal of Chemistry*. 434
2019 (2019). 435
- [39] T.A. Nguyen, T.M.H. Pham, Study on the properties of epoxy composites using fly ash as 436
an additive in the presence of nanoclay: mechanical properties, flame retardants, and 437
dielectric properties, *Journal of Chemistry*. 2020 (2020). 438
- [40] Y. Ma, H. Wan, Y. Ye, L. Chen, H. Li, H. Zhou, J. Chen, In-situ synthesis of size-tunable 439
silver sulfide nanoparticles to improve tribological properties of the polytetrafluoroethylene- 440
based nanocomposite lubricating coatings, *Tribology International*. 148 (2020) 106324. 441
442

Final Revised KSU-1.docx

ORIGINALITY REPORT

10%

SIMILARITY INDEX

9%

INTERNET SOURCES

7%

PUBLICATIONS

1%

STUDENT PAPERS

PRIMARY SOURCES

1	www.researchgate.net Internet Source	2%
2	www.mdpi.com Internet Source	1%
3	www.science.gov Internet Source	1%
4	ejchem.journals.ekb.eg Internet Source	<1%
5	www.hindawi.com Internet Source	<1%
6	arxiv.org Internet Source	<1%
7	www.scientific.net Internet Source	<1%
8	Gelareh Khorgami, Farnaz Solaimany, Seyyed Arash Haddadi, Mohammad Ramezanzadeh, Bahram Ramezanzadeh. "Polyurethanes for Corrosion Protective Coatings", American Chemical Society (ACS), 2023 Publication	<1%

9

Hayder Abbas Sallal, Ahmed Saad Kadhim. "Comparing the Mechanical Behavior of Lamination Resin Reinforced with Two Types of Organic and Inorganic Particles Used in Prosthetic Applications", Key Engineering Materials, 2022

Publication

<1 %

10

C. Kruea-In, S. Eitssayeam, K. Pengpat, G. Rujijanagul, T. Tunkasiri. " Effects of vibro-milling on relaxor ferroelectric behavior and phase transition of lead-free Ba(Zr Ti)O ceramics ", Phase Transitions, 2010

Publication

<1 %

11

journals.sagepub.com

Internet Source

<1 %

12

worldwidescience.org

Internet Source

<1 %

13

Saber-Samandari, S.. "An experimental study on clay/epoxy nanocomposites produced in a centrifuge", Composites Part B, 200701

Publication

<1 %

14

Soumyajit Koley, Abhijit Ghosh, Ashok Kumar Sahu, Ashok Kumar Suri. "Nano-Crystalline Ytria Samaria Codoped Zirconia: Comparison of Electrical Conductivity of Microwave and Conventionally Sintered Samples", Wiley, 2010

Publication

<1 %

15	Submitted to Xiamen University Student Paper	<1 %
16	kbes.journals.publicknowledgeproject.org Internet Source	<1 %
17	dspace.nitrkl.ac.in Internet Source	<1 %
18	scholarbank.nus.edu.sg Internet Source	<1 %
19	Joseph Raj Xavier. "Superior Surface Protection, Mechanical and Hydrophobic Properties of Silanized Tungsten Carbide Nanoparticles Encapsulated Epoxy Nanocomposite Coated Steel Structures in Marine Environment", Silicon, 2022 Publication	<1 %
20	docplayer.net Internet Source	<1 %
21	pubs.rsc.org Internet Source	<1 %
22	vulmbiotech.com Internet Source	<1 %
23	D A Yassen, F M Othman, A A Abdul Hamead. "Preparation and Characterization of CuO/MgO Nano Particles using Sol-Gel	<1 %

Technique", IOP Conference Series: Materials Science and Engineering, 2021

Publication

24	alkej.uobaghdad.edu.iq Internet Source	<1 %
25	bibliotekanauki.pl Internet Source	<1 %
26	dspace.ncl.res.in:8080 Internet Source	<1 %
27	ijmmm.ustb.edu.cn Internet Source	<1 %
28	open.uct.ac.za Internet Source	<1 %
29	www.ijee.ieefoundation.org Internet Source	<1 %
30	"Natural and Synthetic Fiber Reinforced Composites", Wiley, 2022 Publication	<1 %

Exclude quotes Off

Exclude matches Off

Exclude bibliography On